FOREX Publication
Open Access | Rapid and quality publishing
International Journal of Electrical and Electronics Research (IJEER)
Research Article | Volume 13, Issue 1| Pages 01-09| e-ISSN: 2347-470X

Enhanced Performance of E-STATCOM Using Fuzzy Logic Controller for Grid-Connected Wind Systems Under Dynamic Fault Conditions

Srinu Bhukya[1*], T. Murali krishna[2], G. Mallesham[3] and Ch. Anilbharadwaj[4]

[1]*Research scholar, Department of Electrical Engineering, University College of Engineering, Osmania University, Hyderabad, Telangana, India-500007. Email: srinu.bhukya@gmail.com*

[2]*Assoc. Professor, Department of Electrical & Electronics Engineering, Chaitanya Bharati Institute of Technology, Gandipet, Hyderabad, India-500075*

[3]*Professor, Department of Electrical Engineering, University College of Engineering, Osmania University, Hyderabad, Telangana, India-500007*

[4]*Staff Engineer, Embedded DVT, Storage Business Unit, Enphase Solar Energy India (Pvt.) Ltd., Bengaluru, Karnataka, 560017.*

Correspondence: Srinu.bhukya@gmail.com;

ABSTRACT- This Paper introduces an advanced approach to enhancing the efficiency of grid-connected wind cogeneration systems by replacing conventional proportional-integral (PI) controllers with fuzzy logic controllers (FLC) for the Voltage Source Converter (VSC). Integrating renewable energy sources into power grids poses several challenges, particularly in maintaining the stability of the electrical distribution network (EDN). To address these issues, this work employs points of common coupling (CCP) and two-level converters with Dual Active Bridge (DAB) technology to integrate storage modules effectively. The proposed system features an E-STATCOM setup with DAB-based active and reactive power support, enabling simultaneous operation for improved grid stability. FLCs are utilized in place of PI controllers for both the VSC and DAB to enhance efficiency and reliability under varying grid conditions. The wind farm is subjected to diverse fault scenarios to evaluate power and voltage variations, demonstrating the effectiveness of the proposed control strategy. The DAB-based E-STATCOM, controlled by FLC, significantly improves transient voltage stability across multiple fault conditions while maintaining performance comparable to traditional PI controllers. The proposed system's effectiveness has been validated through simulations in the MATLAB/Simulink environment.

Keywords: Renewable Energy Resource (RER), Energy storage based Statcom (EsST), Proportional Integral Controller (PI), Fuzzy Logic Controller (FLC), Dual active bridge (DAB).

ARTICLE INFORMATION

Author(s): Srinu Bhukya, T. Murali krishna, G. Mallesham and Ch. Anilbharadwaj;
Received: 02/12/24; **Accepted**: 15/03/25; **Published**: 30/03/25
E- ISSN: 2347-470X.
Paper Id: IJEER240441
Citation: 10.37391/ijeer.130101
Webpage-link:
https://ijeer.forexjournal.co.in/archive/volume-13/ijeer-130101.html

Publisher's Note: FOREX Publication stays neutral with regard to Jurisdictional claims in Published maps and institutional affiliations.

1. INTRODUCTION

Recent years have seen a sharp increase in the use of wind energy because of lower installation costs and better control technologies. This growth is further accelerated by the transition away from fossil fuels. The development of sustainable energy now heavily relies on wind power. Efficiency and scalability in technology are improving as it develops [1]. In the last thirty years, Wind is one of the most promising renewable energy sources; nevertheless, there are certain technological obstacles to its integration into power systems that affect supply security in terms of dependability, accessibility and the quality of power. The control of wind power is primarily determined by its penetration level, but it is also influenced by load changes, power system size, mix of generation capacity, and degree of system interconnection. As wind power generation becomes more widespread, system operators are becoming more interested in examining how wind power affects the linked electrical system. Grid connection criteria are defined as a result. Dynamic needs, such as voltage dip ride-through capability, have been added to the connection requirements in recent years in addition to steady state issues [2]. The generation of energy based on Renewable Energy Resources (RER) is required due to the decrease in fossil fuel use and rise in energy demand. Utilizing locally accessible resources to meet energy demands is also working as a good approach. Because of its high conversion efficiency, simplicity of use, inexpensive installation costs, and other advantages, wind and solar energy generation is growing at a rate twice as fast as that of other renewable energy sources. However, because wind speed and solar insolation level are stochastic, these resources produce power that varies. The infusion of the variable power generated by the DGs affects the voltage and frequency stability of the current EDN. Designed for this reason, strict adherence to grid

FOREX Publication
Open Access | Rapid and quality publishing
International Journal of
Electrical and Electronics Research (IJEER)
Research Article | Volume 13, Issue 1| Pages 01-09| e-ISSN: 2347-470X

codes is necessary to enhance system stability [3]. Some of the prerequisites for integrating major renewable energy providers into the grid are Q- assistance for voltage stabilization, Active filtering, Smoothing power, Frequency support, Power oscillation damping and Low-voltage Ride through capability [4].

To resolve energy and environmental challenges, the integration of renewable energy sources (RES) based power generation to the grid is essential. These sources, however, can differ widely and be erratic at times. When RER based power generators are linked to the grid, Energy Storage Systems (ESS) provides an adaptable way to reduce their effects [5-7]. For AC transmission and distribution networks, a STATCOM regulates voltage at the point of common coupling (CCP), modifying the voltage profile by supplying capacitive or inductive current to ensure stability [8].

To incorporate DG into the electrical grid, interface converters inject active power; nevertheless, their ratings are limited, making it impossible to comply with grid rules at the common coupling point [9–10]. They need extra systems for reactive power supply and harmonic filtering, and their MPPT operation causes power fluctuations. Active power support can be offered by energy storage systems (ESS)[11-12].Utilization of energy storage systems is limited by their high costs, and power systems are greatly impacted by medium-frequency wind power changes (0.01Hz–1Hz)[13–14].Since it requires less maintenance and requires fewer installation costs than other storage systems, battery storage systems, or BSSs, are the most often used type. Presents an overview of control approaches for using the BSS to integrate renewable energy [15]. In [16], PI controllers set the gains for the control circuit in a E-STATCOM (EsSt) system that combines storage and VAR correction according to real/reactive power demands at the CCP.

There are advantages to integrating VSCs with PI controllers through FLC, but there are drawbacks as well, such as parameter sensitivity, computational complexity, and grid integration, and the nonlinear nature of renewable energy causes poor performance under changing conditions [17–18]. With PI controllers, an EsST, and a DC-DC converter, the study seeks to lower power losses, improve cogeneration efficiency, and illustrate the efficacy of FLC-based tuning in integrating renewable energy [19]. For EsST, a DAB setup offers real/reactive power support [20].

It has been investigated how to achieve the configuration's real/reactive power support through control. The process of adjusting the PI's gains is explained, and the fuzzy controller controls the DAB's output voltage. Section II discusses how the system works to confirm the usefulness of the specified configuration. Section III gives the procedure how to create EsSt and illustrate the architecture and control configuration of the system. Section IV provides a thorough explanation of the simulation results and suggests a course of action for control. Section V deliberates the process of developing the PI controller for DAB. To monitor variations in voltage and power, the power system is exposed to a range of fault circumstances. EsST and DAB's fuzzy logic controller is utilized to increase transient voltage stability in a variety of failure scenarios. Section VI provides a comparison between the EsST and DAB with PI controllers and fuzzy logic controllers.

2. DESCRIPTION OF THE SYSTEM

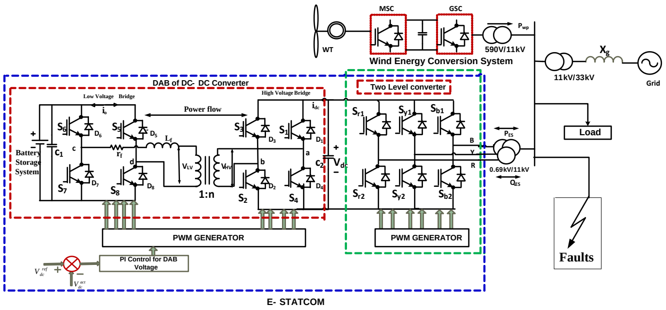

Figure 1. Configuration of E-STATCOM

The grid is connected to wind farms via the point of common coupling, and the effect of wind energy on grid stability particularly in cases of massive wind integrations has been extensively investigated. For stator correction, SCIG-based WECS need capacitor banks, but DFIG-WECS offer bidirectional reactive power assistance, improving voltage stability at grid connection regions [21].

To connect to an AC network, the electronic device uses AC/DC/AC conversion, which improves operational efficiency. The maximum output that the Wind Energy Conversion System (WECS) generates is one megawatt. While the line-side converter (LSC) acts as a rectifier by controlling the fluctuating DC link voltage, the machine-side converter (MSC) provides energy to the DC link to control the speed of the induction machine [22–24].

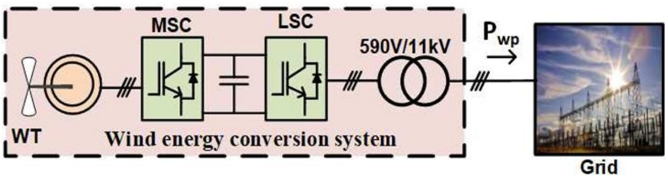

Figure 2. Composition of small-scale wind energy production

The SCIG, which is directly connected to the wind turbine, collects wind power (P_{wp}), while the (back-to-back) BTB converter sends the generator's electrical power (PE) to the grid figure 2. The SCIG-WECS works in two steps. Initially, mechanical energy produced by the wind turbine blades is sent to the SCIG via the shaft, where it is transformed into electrical energy [25]. The mechanical power output of a SCIG wind system can be calculated using the formula below,

$$P_m = \frac{1}{2}\rho A V^3 C_p \ watts \quad (1)$$

If we let,

P=mechanical power in the moving air

ρ=air density, (1.225kg/m^3)

A=area swept by the rotor blades, ($\pi r^2 = 27.58^2\pi$ (m^2))

International Journal of
Electrical and Electronics Research (IJEER)
Research Article | Volume 13, Issue 1| Pages 01-09| e-ISSN: 2347-470X

V=velocity of the air, (12 m/s)
C_p=power co-efficient depending on design of turbine (0.2 to 0.5)
The Appendix contains the complete set of SCIG parameters. WECS generates fluctuating power because of MSC operating MPPT operation. The grid codes are supplied by EsST at the WECS point of common coupling.

3. LAYOUT OF E-STATCOM

Reactive power needs and power quality issues are addressed by the two-level Voltage Source Converter (VSC) used in the EsST design shown in *figure 1*. The VSC adjusts voltage dynamically, compensates for reactive power, and reduces harmonics. This guarantees that the grid runs smoothly and provides higher-quality power. Large-scale renewable energy resource integration into the grid requires compensation of negative sequence current, management and support for active power. By providing electricity when required, the battery storage system satisfies energy demand and maintains a steady flow of energy. It improves system efficiency and facilitates power balancing by connecting to the VSC at DC-link through a low-voltage storage module [16].

3.1. Two level Voltage source converter

A two-level VSC was used to incorporate the battery modules into the alternating current network. The paper next section explains the VSC control principle. A full presentation of the VSC rating can be found in [16]. The BSS is integrated with the grid via a two-level VSC, which offers ancillary services to satisfy grid code requirements.

3.2. Integration of Storage modules

The bi-directional converter that links the VSC and storage modules is described in [26]. The EsSt was first equipped with a boost-type DC-DC converter but due to its shortcomings, Dual Active Bridge (DAB) technology [27], which offers greater conversion ratios and lower switching losses, was adopted. As illustrated in figure 1 [28], DAB converters are superior to Half-Bridge converters in terms of efficiency and EMI reduction, making them perfect for high-power, bidirectional applications.

4. OPERATING PRINCIPLE OF EsST

To achieve effective energy storage and grid integration, this article combines a BESS with a dual active bridge DC-DC converter. As illustrated in figure 1, the EsST system consists of a battery module, DC-DC stage, and DC-AC stage. The VSC control principles are described, and stable power flow management is ensured by Equation (2), which computes the EDN load demand and power support.

$$P_{ES}^{ref} = P_G - P_{wind} \quad (2)$$

P_{wp} stands for the estimated WECS power during the upcoming hour and P_{ES}^{ref} is the active power support by the EsST. When distributed generation is not available, the grid supplies planned power assistance (P_G), which acts as a backup power source to satisfy load demand. The EsST primary goals are to regulate the CCP voltage and reduce variations in the distribution network's actual power usage.

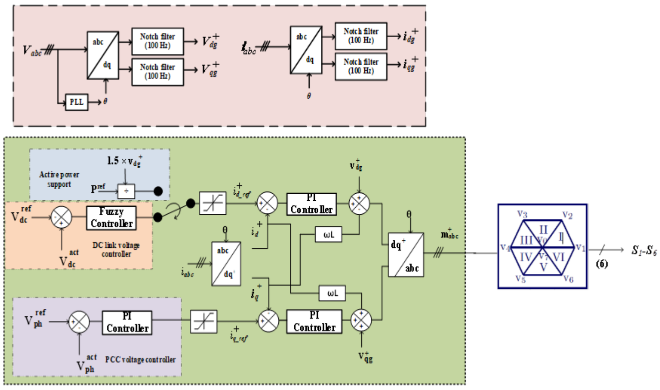

Figure 3. VSC controller supporting grid codes

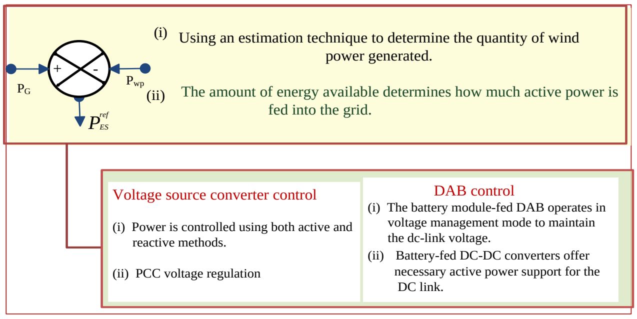

Figure 4. Control of DAB-Fed VSC

The WPCS and CCP communicate via a three-phase, VSC-based STATCOM, which features one PI controller for external DC voltage and two PI controllers for internal current. Grid voltage disturbances in renewable energy systems are frequent, necessitating connected components to provide voltage support. Both symmetrical and asymmetrical grid faults can benefit from the reactive and active current injection that EsST provides to help with voltage regeneration [29].

4.1.VSC Control

The control block for the two-level converter is depicted in figure 3, with elements such as grid synchronization, current regulation, and DC-link voltage control. The i_d and i_q components regulate the real and reactive power support, while the modulation index (m) is modified for both positive and negative sequences. To maintain the required DC-link voltage for STATCOM functioning, the active power controller and DC-link voltage controller work together to control the i_d^{ref} [30].

$$I_q^{ref} = -\frac{Q_{ES}}{1.5 * V_d^*} \quad (3)$$

$$I_d^{ref} = \frac{P_{ES}}{1.5 * V_d^*} \quad (4)$$

The V_d and V_q are the control voltages of current controllers. Active (P_{ES}) and reactive (Q_{ES}) power can be obtained by adjusting i_d^{ref} and i_q^{ref} equations (3) and (4).

The d-axis PI controller processes the (I_d^{ref} -I_d) to generate u_d. By adjusting the i_d, the desired active power can be provided at the CCP by the E-STATCOM. Similarly, q-axis PI-controller processes the (I_q^{ref} -I_q) to generate u_q as shown figure 3. Equation (5) describes how the DC voltage regulator (PI) calculates the I_d^{ref} when it receives the DC voltage error signal.

$$I_d^{ref} = (K_p + \int K_i)(V_{dc}^{ref} - V_{dc}^{act}) \quad (5)$$

Above equation (5), is the DC-Link voltage as measured at the dc-link capacitor $C_{dc\text{-}link}$ is shown by $V_{(dc\text{-}link)}$, whereas the reference dc-link voltage is represented by V_{dc}^{ref} and ^{actual} represented by V_{dc}^{act} is shown figure 3. The expression (K_p+∫K_i) represents a Proportional-Integral (PI) controller gain.

To provide U_dU_q signals, the current regulator (PI) receives these I_d-I_q error signals. The final reference signal generator [19], which produces the reference signal required for the VSC to operate, receives input from the U_dU_q, I_dI_q, and V_dV_q components. Figure 5 below depicts the internal organization of the reference signal generator.

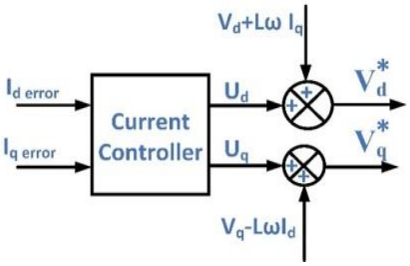

Figure 5. Final generator of V_d*-V_q*

The mathematical representation of the structure is given by equations (6) and (7)

$$V_d^* = U_d + V_d + L\omega I_q \quad (6)$$
$$V_q^* = U_q + V_q - L\omega I_d \quad (7)$$

These final reference voltage signals, V_d*–V_q*, are transformed into "abc" components, which serve as the SPWM (Sinusoidal PWM) technique's reference signals [20].

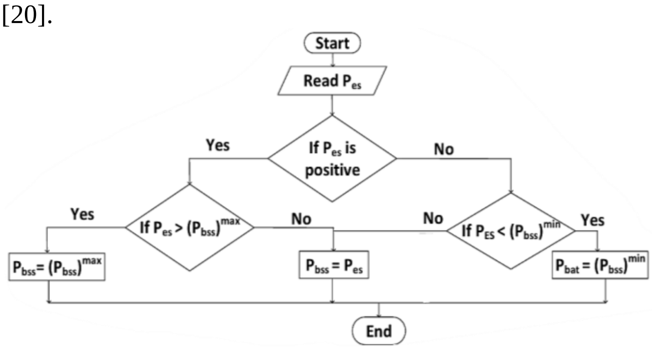

Figure 6. Algorithm of Active power among batteries

The algorithm for P_{ES} distribution begins by identifying the sign of the required active power is shown in figure 6. If the P_{ES} is positive, the storage modules are tasked with supplying the power. The system then checks if the P_{ES} is within the BESS rating, ensuring that P_{ES}<P_{max_bss}. If so, the BESS provides the necessary power; if not, the BESS supplies the maximum allowed power, P_{bss}=P_{max_bss}. Conversely, if the P_{ES} is negative, the storage modules must absorb the power. The system verifies that P_{ES}>P_{min_bss} to ensure the required absorption is within the BESS's capability. If it is, the BESS absorbs the power; otherwise, it absorbs the minimum allowed power, P_{bss}=P_{min_bss}.

4.2.DAB Modelling

The isolation transformer and coupling inductor L connect the two full-bridge circuits of the DAB converter shown in figure 1. The left bridge is connected to the HV DC bus, while the right bridge is connected to the LV battery system. High-frequency square-wave voltages are produced by every bridge, where the HV and LV sides are denoted by V_{HV} and V_{LV}, respectively. With T_S being the switching time and D being the regulated duty ratio, the phase shift between V_{HV} and V_{LV} equals $dT_S/2$ [31-34].In the charging mode for EsST to grid (G2E-STATCOM), the secondary bridge uses a phase delay and a lagging phase shift angle (φ); in the discharging mode (E-STATCOM2G), the primary bridge also employs phase delay and a lagging phase shift angle [35–36].

The input and output voltage levels' magnitudes as well as the phase difference between them determine how much power is transferred.

$$P_o = \left[\frac{nV_{HV}V_{LV}}{2L_sf_s}\right]D(1-D) \quad (8)$$

The DAB's high-frequency transformer's switching frequency and leakage inductance are denoted by the symbol's f_s and L_s (8). For power to flow from the battery module to the DC-link, the phase angle "D" between V_{HV} and V_{LV} must be positive; for reverse power flow, it must be negative [37].

4.3.DAB Control

In order to control PI, the PI controllers adjust output current and are sensitive to variations in DAB's input voltage, while the DAB output voltage is resistant to these variations [38]. A PI controller changes the pulse timing by a phase angle (φ) after comparing the observed DC voltage to V_{dc}^{ref} in the battery current controller, which is depicted in figure 4. With the output voltage managed by the PI controller and dictated by the DC-link voltage (V_{dc}), the DAB's performance is improved by varying the phase shift between the primary and secondary voltages [39].

One way to express the DAB input and output current expressions (9) and (10) are follows from figure 1.

$$i_o = \frac{D(1-D)T_{sw}v_{in}}{L_s} \quad (9)$$
$$i_{in} = \frac{D(1-D)T_{sw}v_o}{nL_s} \quad (10)$$

The state space representation of DAB using the averaging techniques is provided below.

International Journal of
Electrical and Electronics Research (IJEER)
Research Article | Volume 13, Issue 1| Pages 01-09| e-ISSN: 2347-470X

$$\hat{i_o} = g_{od}\hat{D} + g_{ov_{in}}\widehat{v_{in}} \quad (11)$$

$$\hat{i_o} = g_{id}\hat{D} + g_{iv_o}\widehat{v_o} \quad (12)$$

Where $g_{od} = \frac{v_o(1-2D)}{(1-D)DR_o}$, $g_{ov_{in}} = \frac{v_o}{v_{in}R_o}$, $g_{id} = \frac{v_o^2(1-2D)}{v_{in}(1-D)DR_o}$ and $g_{iv_o} = \frac{v_o}{v_{in}R_o}$, In contrast, the relation was presented (13). The phase angle (D) and output voltage of DAB may be determined using equations (11) and (12).

$$\widehat{v_o} = \left(\frac{R_o}{R_o C_o s+1}\right)\left(\frac{v_o(1-2D)}{(1-D)DR_o}\right)\hat{D} \quad (13)$$

Hence from the expression in (13), the output voltage of a DAB can be adjusted with the help of phase angle (D).In [33], the procedure to design the Proportional-Integral controller to operate the DAB has been proposed and the performance of DAB in EsSt application has been explored in [40].

To manage multiple failure scenarios, the operator needs to confirm that voltage support components are performing as expected. Line-to-line (LL), line-line-ground (LLG), three-phase line-to-ground (LLLG), and triple Line (LLL) faults are examples of symmetrical and asymmetrical faults that are frequently present in power system. This approach preserves system dependability and voltage support even in the presence of fault scenarios by mitigating the consequences of both symmetrical and asymmetrical failures [41-42].

5. FUZZY LOGIC CONTROLLER FOR DAB

To improve the efficiency of the EsST DAB is used conventionally, a PI controller is used to maintain DC link voltage as constant. But during dynamic fault conditions the performance of PI controller is poor. Hence an artificial intelligent controller is proposed in this work “figure 7” shows the block diagram of proposed FLC used at DAB which has two inputs and one output which in terms provides modulated pulses to the switches in the DAB.

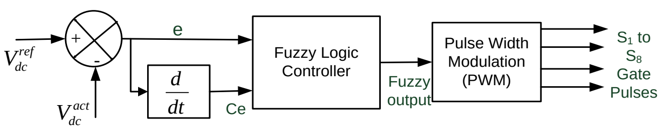

Figure 7. Control structure of FLC

The processes for generating PI gains for DAB are described in [24], while [22] explains the DAB modelling. The error between the reference and measured voltages is used by the PI control module to modify Kp and Ki.

The two inputs give to the FLC are error in the dc-link voltage and change in error in the dc link voltage having five triangular membership functions named given as moderately Negative (-NM), Very Large Negative (-EN), Extremely High Positive (+EP), Positive but Moderate (+PM), and Zero (Z). The output is also having five triangular membership function namely given as moderately Negative (-NM), Very Large Negative (-EN), Extremely High Positive (+EP), Positive but Moderate (+PM), and Zero (Z) then 25 rules are framed as per this output is defuzzyfier with centroid method to produces suitable reference signal for PWM circuit[28].

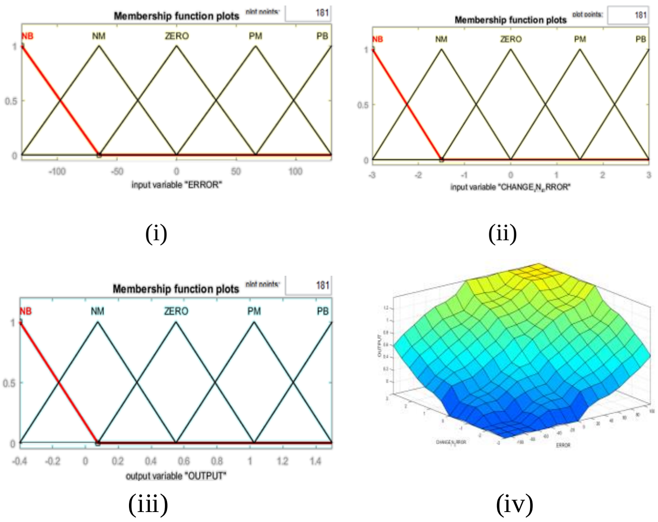

e/ce	-EN	-NM	Z	+PM	+EP
-EN	-EN	-EN	-EN	-NM	Z
-NM	-EN	-EN	-NM	Z	+PM
Z	-EN	-NM	Z	+PM	+EP
+PM	-NM	Z	+PM	+EP	+EP
+EP	Z	+PM	+EP	+EP	+EP

(v)

Figure 8. (i) Memberships of the input error (ii) Memberships of the change in error (iii) Membership functions for output (iv) Surface Viewer layout (v) Fuzzy rules

According to *table 1*, the fuzzy logic controllers employ 25 If-Then rules, and the output signal DAB is quantized into five levels [28]. The ranges of the input variables "error (e)," "change in error (ce)," and "fuzzy output" are -130 to 130, -3 to 3, and -0.4 to 1.5 degrees, respectively [29]. The fuzzy output value is computed using *table 8(v)*. 25-rule set. On a 3D control surface, the roller blind's current position based on measured inputs is displayed, along with the relationship between inputs and output is shown figure 8 [30-32].

6. DISCUSSION ON RESULTS

6.1. Performance of EsST

For the proposed EDN with EsST and WEGS which is shown in *figure 1* is developed in MATLAB simulation environment which is shown in *figure 9*.

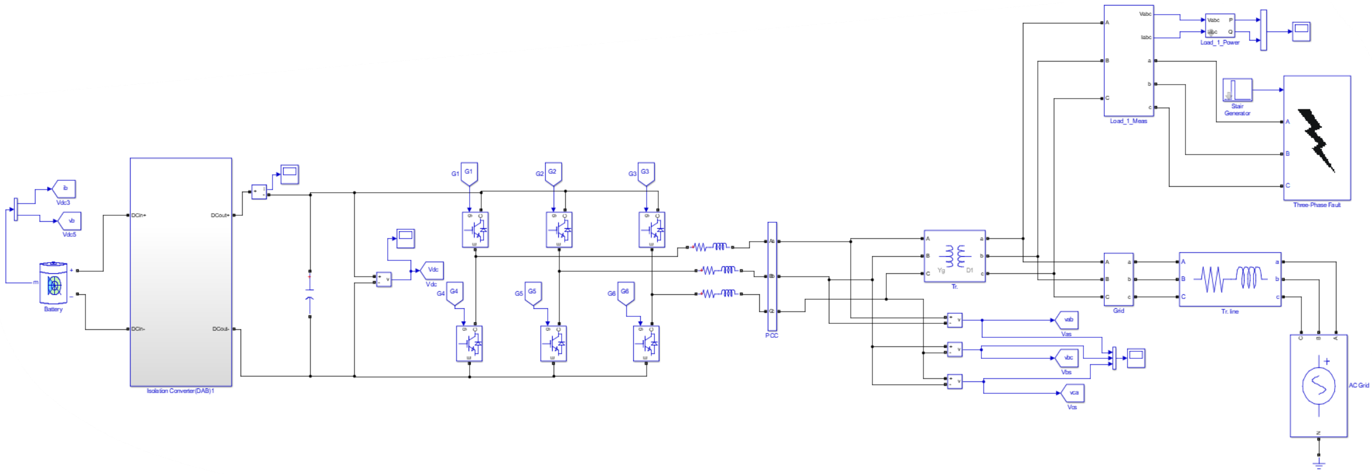

Figure 9. Simulation block diagram of DAB based EsST

As the velocity of wind energy charges, the active power supplied by WEGS changes which is shown in figure 10. The response of EsST for the above variation is also shown in figure 10.

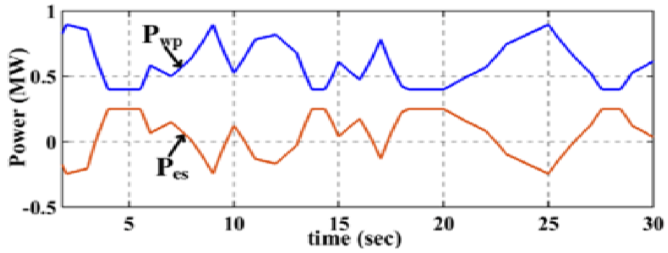

Figure 10. Wind power and EsST power

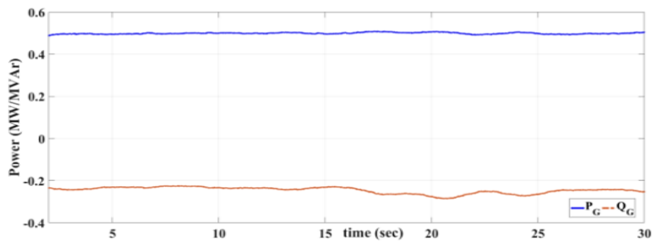

Figure 11. Real and reactive powers at CCP

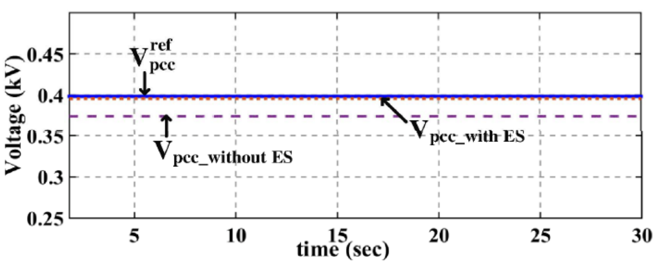

Figure 12. CCP voltage

When EsST is present at the CCP of EDN and allowing for the drawing of a stable power supply from the grid. *Figure 11* displays the CCP's reactive and real power required. Performance of EsST Without EsST, there are variations in the CCP voltage in *figure 12*.

6.2 Performance of E-STATCOM

To observe the performance of the proposed controller the model is tested by creating different dynamic faults namely LG, LL, LLG, LLL and LLLG faults are created near CCP at time is 2second and restored at 2.5second. The simulation results of the proposed circuit are depicted from figure 13 to figure 20.

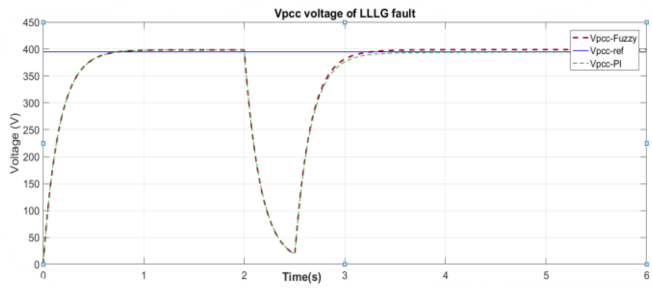

Figure 13. Voltage at CCP during LLLG fault

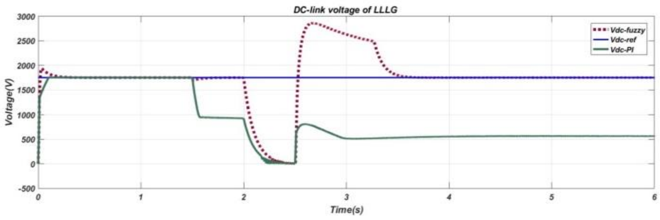

Figure 14. DC link voltage during LLLG fault

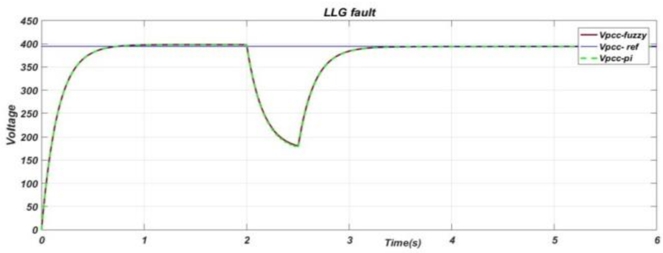

Figure 15. Voltage at CCP during LLG Fault

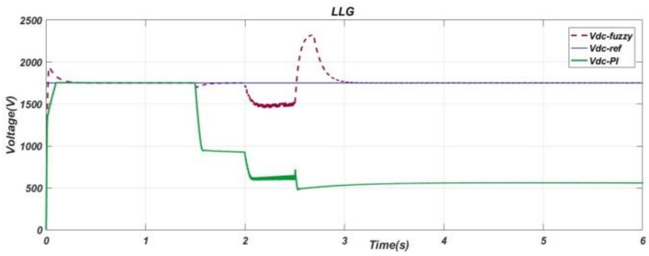

Figure 16. DC link voltage during LLG fault

The DC link voltage is to be maintained at 1750V and the CCP voltage is required to be kept at 400V in all circumstances.

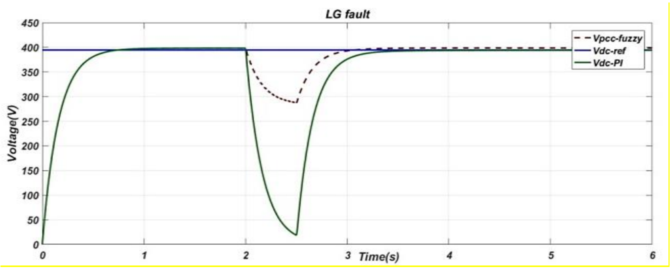

Figure 17. Voltage at CCP during LG fault

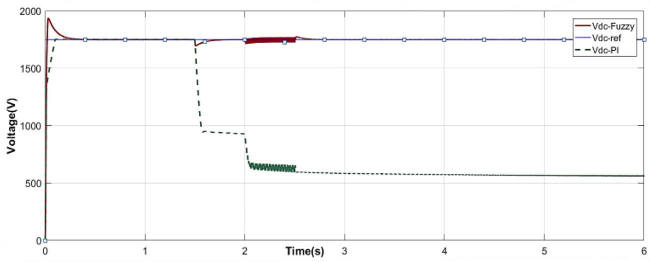

Figure 18. DC link voltage during LG fault

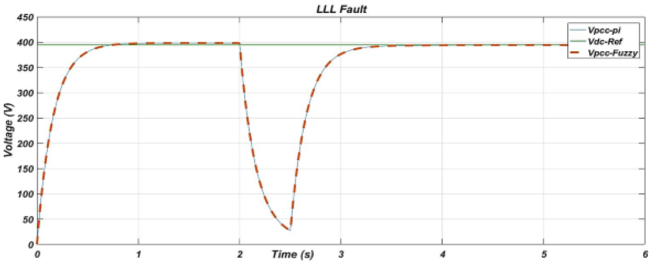

Figure 19. Voltage at CCP during LLL fault

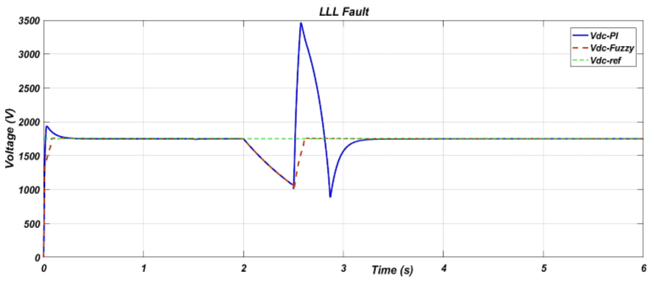

Figure 20. DC link voltage during LLL fault

From figures 13, 15, 17 and 19, it is observed that during various transient faults such as LLG, LLL, and LLLG, the voltage at the CCP is restored quickly using both the PI controller and the Fuzzy Logic Controller (FLC). However, during an LG fault, the dip in the CCP voltage is significantly smaller when using the FLC compared to the PI controller. As a result, the need for Low Voltage Ride Through (LVRT) is lower with the FLC than with the PI controller. Figures 14, 16, and 18 show that, after fault restoration, the DC link voltage is restored with a slight delay using the FLC. In contrast, the PI controller fails to restore the DC link voltage. Figure 20 concludes that while the PI controller can resolve the DC link voltage issue, it does so with a delayed response, unlike the FLC. Therefore, the FLC demonstrates better performance compared to the PI controller.

Table 1. **Steady State error of DC link voltage**

S. No.	Type of Fault	Steady State error	
		PI controller	Fuzzy controller
1	LLLG	1250V	0V
2	LLG	1202V	0V
3	LG	1150V	0V
4	LLL	0V	0V

CONCLUSION

This study suggests that the voltage/frequency of EDN, which is dominated by renewable energy, be supported by the EsST architecture. To regulate the voltage at Common coupling and to provide a constant real power flow to the distribution transformer, the EsST provides the required real and reactive power. To maintain steady operation, the VSC's dc-link voltage is regulated by the DAB controller. To validate the performance using EsST, the distributed generation EDN has been modeled in MATLAB. The outcomes of the simulation indicate that the DC link voltage and CCP voltage can be regulated via the EsST and mitigating fluctuations in active and reactive powers. It can be shown from the simulation results that the proposed fuzzy controller provides better response than PI controller.

To improve system capability and performance, simulation results of the power system using EsST under various faults are conducted. PI controllers and FLCs are two distinct controllers that are used to evaluate the EsST's performance. A comparison investigation of the two distinct controllers' performances in unbalanced scenarios. The outcome shows that, depending on the situation, the EsST with FLC might enhance the power system and perform better than the PI controller.

REFERENCES

[1]. Global Wind Energy Council (GWEC), *Global Wind EnergyOutlook2017*. [Online]. Available: http://www.gwec.net.
[2]. B. Rona and Ö. Güler, "Power system integration of wind farms and analysis of grid code requirements," *Renewable and Sustainable Energy Reviews*, vol. 49, pp. 100–107, 2015.
[3]. A. G. Shaik and O. P. Mahela, "Comprehensive overview of grid interfaced wind energy generation systems," Renewable and Sustainable Energy Reviews, vol. 57, pp. 260-281, 2016.

[4]. V. Khare, S. Nema, and P. Baredar, "Solar–wind hybrid renewable energy system: A review," Renewable and Sustainable *Energy Reviews*, vol. 58, pp. 23–33, 2016.

[5]. B. Rona and Ö. Güler, "Power system integration of wind farms and analysis of grid code requirements," *Renewable and Sustainable Energy Reviews*, vol. 49, pp. 100–107, 2015.

[6]. C. Luo, H. Banakar, B. Shen, and B. Ooi, "Strategies to smooth wind power fluctuations of wind turbine generators," *IEEE Transactions on Energy Conversion*, vol. 22, pp. 341-349, Jun. 2007.

[7]. W. Li, G. Joos, and C. Abbey, "Wind power impact on system frequency deviation and an ESS based power filtering algorithm solution," *Power Systems Conference and Exposition (PSCE '06)*, pp. 2077-2084, 2006.

[8]. Y. Zhu, H. Zang, and L. Cheng, "Output power smoothing control for a wind farm based on the allocation of wind turbines," *Applied Sciences*, vol. 8, no.980, 2018. [Online]. Available:https://www.webofscience.com/wos/alldb/full-record/WOS:000436488000139.

[9]. J. O. Petinrin and M. Shaaban, "Impact of renewable generation on voltage control in distribution systems," *Renewable and Sustainable Energy Reviews*, vol. 65, pp. 770-783, 2016.

[10]. S. P. Jaiswal, S. Lata, S. Singh, S. K. Singh, and J. Singh, "Operating Strategies Optimization of STATCOM for Improvement of Voltage Profile," *2021 International Conference on Computing, Communication, and Intelligent Systems (ICCCIS)*, Greater Noida, India, 2021, pp. 840-844, doi: 10.1109/ICCCIS51004.2021.9397120.

[11]. O. K. Shinde and V. R. S. V. B. Pulavarthi, "STATCOM converters and control: A review," *2017 International Conference on Data Management, Analytics and Innovation (ICDMAI)*, Pune, India, 2017, pp. 145-151, doi: 10.1109/ICDMAI.2017.8073500.

[12]. J. O. Petinrin and M. Shaaban, "Impact of renewable generation on voltage control in distribution systems," *Renewable and Sustainable Energy Reviews*, vol. 65, pp. 770-783, 2016.

[13]. M. I. Mosaad, H. S. M. Ramadan, M. M. Aljohani, F. El-Naggar, and S. S. M. Ghoneim, "Near optimal PI controllers of STATCOM for efficient hybrid renewable power system," *IEEE Access*, vol. 9, pp. 34119–34130, 2021. [Online]. Available: https://doi.org/10.1109/ACCESS.2021.3058081.

[14]. Z. Shi, W. Wang, Y. Huang, P. Li, and L. Dong, "Simultaneous optimization of renewable energy and energy storage capacity with the hierarchical control," *CSEE Journal of Power and Energy Systems*, vol. 8, no. 1, 2022.

[15]. L. M. Silva de Siqueira and W. Peng, "Control strategy to smooth wind power output using battery energy storage system: A review," *Journal of Energy Storage*, vol. 91, pp. 1-11, 2018.

[16]. A. Bharadwaj, S. Maiti, N. Dhal, and S. Chakraborty, "Control of Two-Level Converter based STATCOM with Battery and Ultracapacitor," *Proceedings of National Power Electronics Conference (NPEC)*, pp. 1-6, 2019.

[17]. J. C. Basilio and S. R. Matos, "Design of PI and PID controllers with transient performance specification," *IEEE Transactions on Education*, vol. 45, no. 4, pp. 364-370, Nov. 2002, doi: 10.1109/TE.2002.804399.

[18]. R. Ebrahimi, V. Eslampanah, H. M. Kojabadi, M. Azizian, N. N. Esfetanaj, and D. Zhou, "A Robust Fuzzy-based Control Technique for Wind Farm Transient Voltage Stability Using SVC and STATCOM: Comparison Study," *2020 22nd European Conference on Power Electronics and Applications (EPE'20 ECCE Europe)*, Lyon, France, 2020, pp. P.1-P.5, doi: 10.23919/EPE20ECCEEurope43536.2020.9215750.

[19]. S. Bhukya, A. Bharadwaj, M. K. T, N. V. P. Babu, and G. Mallesham, "Control and Performance Analysis of Multifunctional Two Level STATCOM fed with Battery Storage System," *2022 Second International Conference on Power, Control and Computing Technologies (ICPC2T)*, Raipur, India, 2022, pp. 1-6, doi: 10.1109/ICPC2T53885.2022.9777063.

[20]. S. Bhukya, A. Bharadwaj, M. K. T, N. V. P. Babu, and S. Maiti, "Performance Evaluation of Dual Active Bridge Converter for Energy Storage Integration With STATCOM," *2022 Second International Conference on Power, Control and Computing Technologies (ICPC2T)*, Raipur, India, 2022, pp. 1-6, doi: 10.1109/ICPC2T53885.2022.9776792.

[21]. K. Z. Heetun and S. H. A. Abdel Aleem, "Voltage stability analysis of grid-connected wind farms with FACTS: Static and dynamic analysis," *IET Renewable Power Generation*,vol.10,no.2,pp.208-217,2016.[Online].Available: https://doi.org/10.1080/23317000.2015.1128369.

[22]. Heier, *Grid Integration of Wind Energy Conversion System*, Chichester, UK: John Wiley & Sons Ltd., 1998.

[23]. G. C. Konstantopoulos and A. T. Alexandridis, "Full-Scale Modeling, Control, and Analysis of Grid-Connected Wind Turbine Induction Generators with Back-to-Back AC/DC/AC Converters," *IEEE Transactions on Emerging Topics in Power Electronics*, vol. 2, no. 4, pp. 739-748, Dec. 2014.

[24]. A. G. Abo-Khalil and D. Lee, "MPPT Control of Wind Generation Systems Based on Estimated Wind Speed Using SVR," *IEEE Transactions on Industrial Electronics*, vol. 55, no. 3, pp. 1489-1490, March 2008.

[25]. W. J. Zhu, W. Z. Shen, E. Barlas, F. Bertagnolio, and J. N. Sørensen, "Wind turbine noise generation and propagation modeling at DTU Wind Energy: A review," *Renewable and Sustainable Energy Reviews*, vol. 88, pp. 133-150, May 2018. https://doi.org/10.1016/j.rser.2018.02.029.

[26]. J. Xu, "An analytical technique for the analysis of switching DC-DC converters," *1991 IEEE International Symposium on Circuits and Systems (ISCAS)*, 1991, pp. 1212-1215 vol.2.

[27]. Z. Wang, Y. Wang, and Y. Rong, "Design of closed-loop control system for a bidirectional full bridge DC/DC converter," *Applied Energy*, vol. 194, pp. 617-625, 2017.

[28]. U. Vuyyuru, S. Maiti, and C. Chakraborty, "Active power flow control between DC microgrids," *IEEE Transactions on Smart Grid*, vol. 10, no. 5, pp. 1949-1957, Sept. 2019.

[29]. S. Bhukya, T. M. Krishna, G. Mallesham, and C. A. Bharadwaj, "Design and performance evaluation of fuzzy controller-based energy storage enabled STATCOM for electrical distribution network," *Journal of Electrical Systems*, vol. 20, no. 3, pp. [page numbers], 2024. [Online]. Available: https://doi.org/10.52783/jes.2986.

[30]. C. A. Busada, S. G. Jorge, and J. A. Solsona, "A Synchronous Reference Frame PI Current Controller with Dead Beat Response," *IEEE Transactions on Power Electronics*, vol. 35, no. 3, pp. 3097-3105, March 2020.

[31]. S. M. Tripathi, A. N. Tiwari, and D. Singh, "Optimum design of proportional-integral controllers in grid-integrated PMSG-based wind energy conversion system," *International Transactions on Electrical Energy Systems*, vol. 26, no. 6, pp. 1006–1031, 2016. https://doi.org/10.1002/etep.2120.

[32]. B. Singh and S. Arya, "Design and control of a DSTATCOM for power quality improvement using cross correlation function approach," *International Journal of Engineering, Science and Technology*, vol. 4, no. 1, pp. 1-11, Dec. 2012.

[33]. S. M. Tripathi and P. J. Barnawal, "Design and control of a STATCOM for non-linear load compensation: A simple approach," *Electrical, Control and Communication Engineering*, vol. 14, no. 2, pp. 172-184, Nov. 2018. [Online]. Available: https://doi.org/10.2478/ecce-2018-0021.

[34]. M. N. Kheraluwala, R. W. Gascoigne, D. M. Divan, and E. D. Baumann, "Performance characterization of a high-power dual active bridge DC-to-DC converter," *IEEE Transactions on Industry Applications*, vol. 28, no. 6, pp. 1294-1301, Dec. 1992.

[35]. R. Jatoth and B. Mangu, "Grid-Tied Solar Power Sharing with V2G and G2V Power Exchange with Dual Bridge Integrated Electrical Vehicle," International Journal of Electrical and Electronics Research, vol. 11, no. 1, pp. 192-201, 2024. DOI: 10.37391/IJEER.110127

[36]. S. Thomas, M. Stieneker, and R. W. De Doncker, "Development of a modular high-power converter system for battery energy storage systems," *Proceedings of the 14th European Conference on Power Electronics and Applications (EPE)*, 2011, pp. 1-10.

[37]. A. R. Rodriguez Alonso, J. Sebastian, D. G. Lamar, M. M. Hernando, and A. Vazquez, "An overall study of a Dual Active Bridge for bidirectional DC/DC conversion," *Proceedings of IEEE Energy Conversion Congress and Exposition*, pp. 1129-1135, 2010.

[38]. S. Tiwari, O. Hanif, and S. Sarangi, "Modeling and control of Dual Active Bridge by Fractional order controllers," *Proceedings of International Conference on Power Electronics, Control and Automation (ICPECA)*, pp. 1-6, 2019.

[39]. Z. Wang, Y. Wang, and Y. Rong, "Design of closed-loop control system for a bidirectional full bridge DC/DC converter," *Applied Energy*, vol. 194, pp. 617-625, 2017.

[40]. A. K. Jain and R. Ayyanar, "PWM control of dual active bridge: Comprehensive analysis and experimental verification," *IEEE*

Transactions on Power Electronics, vol. 26, no. 4, pp. 1215-1227, April 2011.
[41]. R. Niveditha and A. Jeevanandham, "Damping out system oscillations in power system using UPFC for various faults," *2017 International Conference on Advances in Electrical Technology for Green Energy (ICAETGT)*, Coimbatore, India, 2017, pp. 135-138, doi: 10.1109/ICAETGT.2017.8341471.
[42]. M. A. Soliman, H. M. Hasanien, H. Z. Azazi, E. E. El-Kholy and S. A. Mahmoud, "An Adaptive Fuzzy Logic Control Strategy for Performance Enhancement of a Grid-Connected PMSG-Based Wind Turbine," in *IEEE Transactions on Industrial Informatics*, vol. 15, no. 6, pp. 3163-3173, June 2019, doi: 10.1109/TII.2018.2875922.

APPENDIX

Table 2. System rating for battery storage

S. No.	Specification	Value
1	The battery module's capacity	0.175 MWh
2	Battery modules are used to support active power.	0.35 MW
3	The nominal voltage of the battery module	1.35 kV
4	Output voltage of a DC-DC converter	1.75kV
5	Duty ratio(D)	0.229
6	Each battery's voltage	3.5V
7	Number of interconnected series cells	386
8	Discharge current through each battery	100A
9	Number of parallel battery modules	3
10	The DC-DC converter filter inductance	14.82mH

Table 3. Parameters of E-STATCOM

S. No.	Specification	Value
1	The capacity of the converter (S)	0.75 MVA
2	Active Power Capacity	0.35 MW
3	Duration of active power support	30 minutes
4	DC link voltage	1.75 kV
5	Line voltage	0.69 kV
6	capacitance of the DC-link	25 µf
7	Inductance of the filter	1.0 mH
8	Transformer voltage rating	0.69kV/11kV

Table 4. Wind plant parameters

S. No	Specification	Value
1	RMS Line-Line voltage at the bus for collections	11 kV
2	Capacity of the SCIM	1.5 MW
3	The SCIM's rated voltage	590 V
4	Capability of MSC and GSC	1.5 MW

Table 5. Injecting power into the grid

S. No	Specification	Value
1	Active power injection into the grid	0.625MW
2	Reactive power support at CCP	0.35 MVAr
3	The load at the CCP	100kVA, 0.9 p.f

Table 6. DAB's parameters

S. No.	Specification	Value
1	Parameter Value All battery modules' capacities	0.9 MWh
2	Support of active power from Battery modules	0.18 MW
3	The battery terminal voltage	0.4 kV
4	Voltage supplied by DC-DC converter	1.5 kV
5	A DAB's filter inductance	9.722 uH
6	Switching frequency	5 kHz

Author(s) Biography

Srinu Bhukya received the B.Tech in Electrical and Electronics Engineering from the Jayamukhi Institute of Technological Sciences, JNTU, Hyderabad, Telangana. And the M.Tech degree in Power Electronics from Aurora Engineering college, JNTU, Hyderabad. Currently he is a Ph.D scholar in the Electrical Engineering Department, University College of Engineering (UCE), Osmania University, Hyderabad, Telangana. His research interests are Power Electronics & Drives, renewable energy resources and HVDC.
Email: srinu.bhukya@gmail.com

T Murali Krishna received UG degree from the Institution of Engineers (India), Kolkata in 2001, M. Tech in Electrical Power Systems, and PhD from JNTUA, Anantapuramu, Andhra Pradesh in 2005 and 2016, respectively. He is presently working at Chaitanya Bharathi Institute of Technology as an Associate Professor in the Department of EEE. His research interests include Power Electronics, FACTS, Wavelets, and Renewable Energy Integration etc.
Email: tmurali5@gmail.com

Prof.G. Mallesham received the B. E degree in electrical engineering from the University College of Engineering, O. U, Hyderabad, M.Tech degree in control and instrumentation engineering from IIT Delhi, and the Ph.D in Electrical Engineering Department, IIT Delhi. He joined the Department of Electrical Engineering, University College of Engineering, O.U, Hyderabad, as Assistant Professor in 2002 and is currently working as Professor. His research interests are system modeling, control and automation, soft computing, distribution generation, renewable energy, and smart microgrid.
Email: drgm@osmania.ac.in

Anil Bharawdaj.Ch received B.Tech degree in electrical engineering from JNTU Kakinada, India in 2009 and M.Tech degree in Power electronics & Drives from National Institute of Technology, Kurukshetra, India in 2013 and obtained Ph.D. from Department of Electrical Engineering, Indian Institute of Technology, Kharagpur in 2020, India. At present, he's working as a Staff Engineer in the Storage Business Unit of Enphase Solar Energy Pvt (Ltd). India. His research interests are multilevel converters, integration of battery storage systems, control and renewable power generation.
Email: anilbharadwajc@gmail.com